



## Experimental radiobiology

## Glycolytic metabolism and tumour response to fractionated irradiation

Ulrike G.A. Sattler<sup>a,1</sup>, Sandra S. Meyer<sup>a,1</sup>, Verena Quennet<sup>a,2</sup>, Christian Hoerner<sup>a</sup>, Hannah Knoerzer<sup>a</sup>, Christian Fabian<sup>a</sup>, Ala Yaromina<sup>b</sup>, Daniel Zips<sup>b</sup>, Stefan Walenta<sup>a</sup>, Michael Baumann<sup>b,c,d</sup>, Wolfgang Mueller-Klieser<sup>a,\*</sup>

<sup>a</sup> Institute of Physiology and Pathophysiology, University Medical Center of the Johannes Gutenberg University Mainz, Germany; <sup>b</sup> Department of Radiation Oncology; <sup>c</sup> Experimental Centre; and <sup>d</sup> OncoRay-Centre for Radiation Research in Oncology, Technische Universität Dresden, Germany

## ARTICLE INFO

## Article history:

Received 26 June 2009

Received in revised form 18 September 2009

Accepted 4 November 2009

Available online 28 December 2009

## Keywords:

Metabolic bioluminescence imaging  
Human tumour xenograft  
Fractionated irradiation  
Local tumour control  
Tumour glycolysis  
Human head and neck squamous cell carcinomas

## ABSTRACT

**Background and purpose:** To study whether pre-therapeutic lactate or pyruvate predict for tumour response to fractionated irradiation and to identify possible coherencies between intermediates of glycolysis and expression levels of selected proteins.

**Materials and methods:** Concentrations of lactate, pyruvate, glucose and ATP were quantified via bioluminescence imaging in tumour xenografts derived from 10 human head and neck squamous cell carcinoma (HNSCC) lines. Tumours were irradiated with 30 fractions within 6 weeks. Expression levels of the selected proteins in tumours were measured at the mRNA and protein level. Tumour-infiltrating leucocytes were quantified after staining for CD45.

**Results:** Lactate but not pyruvate concentrations were significantly correlated with tumour response to fractionated irradiation. Lactate concentrations *in vivo* did not reflect lactate production rates *in vitro*. Metabolite concentrations did not correlate with GLUT1, PFK-L or LDH-A at the transcriptional or protein level. CD45-positive cell infiltration was low in the majority of tumours and did not correlate with lactate concentration.

**Conclusions:** Our data support the hypothesis that the antioxidative capacity of lactate may contribute to radioresistance in malignant tumours. Non-invasive imaging of lactate to monitor radiation response and testing inhibitors of glycolysis to improve outcome after fractionated radiotherapy warrant further investigations.

© 2009 Elsevier Ireland Ltd. All rights reserved. Radiotherapy and Oncology 94 (2010) 102–109

Despite some controversial opinions [1,2], it is generally accepted that malignant transformation is associated with an increase in glycolytic flux, and that this increase is mainly caused by an up-regulated expression of membrane-based glucose transporters, glycolytic enzymes and proteins with a regulatory impact on glycolytic enzymes [3–5]. As a consequence of these oncogenic metabolic alterations, tumour cells are permanently producing lactate even in the presence of oxygen, a phenomenon which is known as “aerobic glycolysis” or the “Warburg effect” [6].

Early studies in 1990s using bioluminescence imaging had already revealed a positive correlation between the extent of lactate accumulation in primary malignancies and the incidence of metastasis in carcinomas of the uterine cervix [7] and of the head and neck [8]. In subsequent independent studies on these tumour entities, it was found that overall as well as recurrence-free survival,

predominantly after combined radio-/chemotherapy, was significantly reduced in patients with high compared to those with low lactate concentrations within primary tumours; this was true for the pre-therapeutic lactate concentration of the primary tumours with identical clinical staging and pathohistological grading at first diagnosis [9,10]. It has been clearly documented that lactate and pyruvate [11,12] effectively scavenge reactive oxygen species (ROS), and that ROS are required for the fixation of radiation-induced DNA damage [13].

This may imply that a high glycolytic turnover rate might be associated with radioresistance, and that the monitoring of antioxidative glycolytic metabolites, such as pyruvate and lactate, may allow to predict radiation response of individual tumours. In fact, in a recent study by our group on five xenografted human head and neck squamous cell carcinomas (HNSCCs) steady-state pre-therapeutic lactate concentration was positively correlated with local tumour control after fractionated irradiation [14].

The current study was performed to extend the preceding investigations on five tumour lines to another five HNSCC lines in an independent experimental study including different investigators, instruments and biochemical approaches. The focus of the present study was to investigate the impact of pyruvate on radiation

\* Corresponding author. Address: Institute of Physiology and Pathophysiology, University Medical Center of the Johannes Gutenberg University Mainz, Duesbergweg 6, 55128 Mainz, Germany.

E-mail address: wolfgang.mueller-klieser@uni-mainz.de (W. Mueller-Klieser).

<sup>1</sup> Shared first authorship.

<sup>2</sup> Present address: Radiation Biology and DNA Repair, Technische Universität, Darmstadt, Germany.

response. Although often discussed and hypothesised, to our knowledge this is the first systematic experimental study on pyruvate and radiosensitivity in tumours *in vivo*. We hypothesise that lactate and/or pyruvate correlate with tumour response to fractionated irradiation. To elucidate underlying molecular mechanisms of inter-tumoural heterogeneity in lactate concentration, glycolytic enzymes on the transcriptional and proteomic level, cellular lactate production rates and tumour-associated leucocytes were studied.

## Materials and methods

### Tumour models and irradiation

Ten established human head and neck squamous cell carcinoma (HNSCC) lines (CAL-33; FaDu; HSC-4; SAS; UT-SCC-5; UT-SCC-8; UT-SCC-14; UT-SCC-15; UT-SCC-45; XF354) were xenografted in nude mice. Tumour characteristics including radiation sensitivity, hypoxia and parameters of the metabolic microenvironment have been published previously [15–18]. HSC-4 tumours evoked significant residual immune response [16]. Briefly, tumours were transplanted subcutaneously into the right hind-leg of NMRI (nu/nu) nude mice which had received whole body irradiation with 4 Gy (200 kV X-rays, 0.5 mm Cu filter, 1 Gy/min) 2 days before tumour transplantation. When grown to a diameter of 7 mm, tumours were either excised for histological studies and bioluminescence imaging or irradiated with 30 graded fractions within 6 weeks. Local tumour control was evaluated 120 days after fractionated irradiation. Tumour control data were fitted using a Poisson model and the TCD<sub>50</sub>, i.e., the radiation dose necessary to control 50% of the tumours, was calculated [19].

### Quantitative bioluminescence imaging of metabolites

Cryosections parallel to those used for immunohistochemistry served for quantitative bioluminescence imaging of lactate, glucose, pyruvate and ATP. The latter metabolite indicated appropriate tissue sampling, and it allowed, besides haematoxylin and eosin (H&E) staining, for the discrimination between vital and necrotic tumour regions. The technique of bioluminescence imaging has been described in detail previously [20,21]. Briefly, cryosections were brought into contact with an enzyme solution that linked the metabolite of interest to bacterial luciferase or firefly luciferase, respectively, in a quantitative manner. This leads to light emission with the intensity being proportional to the local metabolite concentration. Using appropriate standards, i.e., various concentrations of the metabolite of interest dissolved in Tissue-Tek O.C.T. (Sakura Finetek GmbH, Staufen, Germany) or in 0.1 M phosphate buffer with 9% polyvinyl alcohol and 4.5% polyethylene glycol, light intensity was calibrated with regard to local metabolite concentration in  $\mu\text{mol/g}$  tissue. Data acquisition was restricted to vital tumour regions by interactive computerised image analysis through overlaying metabolite images with the images of parallel sections stained with H&E and/or an anti-mouse antibody. ATP, lactate and glucose concentrations of five tumour lines (XF354, UT-SCC-14, UT-SCC-15, FaDu and UT-SCC-5) have been published earlier [14]. The tumour lines CAL-33 and SAS were measured and analysed as described in this previous study. Detection of light emission of the tumour lines UT-SCC-8, UT-SCC45 and HSC-4 was performed with a new 16-bit CCD camera system (iXon<sup>EM</sup> + DU-888, Andor Technology PLC, Belfast, Northern Ireland). In these cases, a modified enzyme solution according to Mueller-Klieser & Walenta [20] was used for lactate measurements: 35 mM glutamate, 20 mM NAD, 0.25 mM FMN, 0.4 mM 1,4-dithiothreitol, 6 mM decanal, 200 U ml<sup>-1</sup> lactate dehydrogenase, 50 U ml<sup>-1</sup> glutamate-pyruvate transaminase, 3.6 U ml<sup>-1</sup> NAD(P)H-FMN-oxidoreductase and 0.0135 U ml<sup>-1</sup> luciferase in 0.1 M phosphate buffer.

### Reverse transcription and real-time PCR assay

RNA expression was determined in xenografted tumours with a quantitative real-time PCR approach. Total RNA was extracted from tumour samples using the RNeasy Mini Kit (QIAGEN, Hilden, Germany) including DNA digestion according to the manufacturer's protocol. RNA integrities were verified on formaldehyde gels to monitor 18S/28S rRNA ratios. RNA qualities and quantities were determined photometrically. For reverse transcription of mRNAs the Reverse-iT<sup>TM</sup> 1st Strand Synthesis Kit (ABgene, Hamburg, Germany) was used. Quantitative PCRs ran in triplicates using a 7300 real-time PCR system with TaqMan<sup>®</sup> Universal Master Mixes and highly specific TaqMan<sup>®</sup> Gene Expression Assays on Demand (Applied Biosystems, Foster City, CA, USA). For quantification, the comparative C<sub>T</sub> method ( $\Delta\Delta C_T$ ) was used with hydroxymethylbilane synthase (hmbs) as reference gene and an independent FaDu cell sample as calibrator. The primer efficiency of hmbs which is not involved in the glycolytic pathway has been checked to be the same as that of the glycolysis-related genes of interest in the calibrator cells, and a recent publication supports the validity of using hmbs as a reference gene in HNSCC [22].

### Western blot

Protein extracts were kindly provided by Dr. Christine Bayer (Munich, Germany). Details on protein extraction and determination of concentrations have been published previously [18]. Sample aliquots of 2.5  $\mu\text{g}$  of protein extract were resolved by sodium dodecyl sulphate–polyacrylamide gel electrophoresis. The proteins were electrotransferred onto an activated Immobilon-FL PVDF membrane (Millipore GmbH, Schwalbach, Germany). Analysis was performed by the Odyssey infrared imaging system (LI-COR Biosciences GmbH, Bad Homburg, Germany). Briefly, the polyvinylidene difluoride (PVDF) membrane was blocked with blocking buffer (Rockland, Gilbertsville, PA, USA) and incubated with a mixture of the primary antibodies against LDH-A and  $\alpha$ -tubulin (Abcam, Cambridge, UK). After washing steps with PBS-T, the membrane was incubated with a mixture of the fluorescence coupled secondary donkey anti-sheep Alexa680 (Molecular Probes Inc., Eugene, OR, USA) and donkey anti-rabbit IRDye800 (Rockland, Gilbertsville, PA, USA) antibodies. After several washing steps with PBS-T and PBS, an image of the membrane was acquired with the Odyssey infrared imaging system and was analysed by the Application Odyssey Software 2.1.12.

### Immunohistochemistry

For immunohistological staining of CD45, 10  $\mu\text{m}$  tumour sections were air-dried over night and fixed with acetone. Tumour sections were blocked with 2% skimmed milk powder in PBS, incubated with the primary antibody against CD45 (Abcam, Cambridge, UK) and subsequently with peroxidase-coupled secondary antibody (goat anti-rat, Dianova GmbH, Hamburg, Germany). Detection of positive antibody binding was performed with 3,3'-diaminobenzidine (DAB<sup>+</sup>) substrate (DAKO GmbH, Hamburg, Germany). Three investigators independently assessed the degree of staining in the tumour tissue in four categories (0: no CD45-positive cells, 1: single positive cells, 2: several CD45-positive cells or small clusters of cells, 3: CD45-positive cells in larger clusters). For each tumour line the numbers of sections in each category were summed up, and the median was calculated.

### Determination of the pimonidazole hypoxic fraction (pHF)

Tumour hypoxia was determined using pimonidazole labelling as described in [16]. In brief, 1 h before tumour excision, 0.1 mg/g body weight of pimonidazole (Natural Pharmacia International,

Belmont, MA, USA) was injected intraperitoneally. Excised and shock frozen tumours were sliced in serial sections. Cryosections adjacent to those used for pimonidazole detection served for bioluminescence imaging and histological staining with H&E. Pimonidazole binding was quantified by semi-automated computerised image analysis. In each section the pimonidazole hypoxic fraction (pHF), i.e., the ratio of the area of positive pimonidazole staining and vital tumour area, was derived. pHF values for the 10 HNSCC lines have been published previously in [14,15,17,23].

#### Lactate production in vitro

To measure the kinetics of lactate production of nine HNSCC cell lines, cells were seeded in six-well flat-bottomed plates (Greiner Bio-One, Frickenhausen, Germany) in DMEM high glucose (4.5 g/l) supplemented with 10% FCS, 10 mM HEPES, 2 mM L-glutamine, 1 mM sodium pyruvate and non-essential amino acids (PAA Laboratories GmbH, Coelbe, Germany). After 3 days and at 80% confluence, the medium was changed, and medium supernatant samples were taken at 0 and 24 h. Deproteinized medium supernatants were analysed with a commercial photometric assay kit (r-biopharm, Darmstadt, Germany) in triplicates according to the manufacturer's instructions. Lactate concentrations were norma-

lised to cell volumes which were assessed by an automatic cell counter (CASY Technology, Reutlingen, Germany).

#### Statistics

In general, 3–7 sections from central regions of 11–13 tumours for each of the 10 lines investigated were used for the quantification of metabolites. Consequently, averaging the mean values of vital tumour regions for each tumour resulted in 11–13 individual mean metabolite concentrations for each of the 10 tumour lines. From these data tumour line-associated statistical parameters were derived, such as mean, median, minimum and maximum values, as well as the 25% and 75% percentiles. These values were displayed as box and whiskers plots for all metabolites and cell lines investigated. Mean ( $\pm$ SD) tumour line-specific data were correlated by linear regression or Spearman rank order correlation analyses, respectively. Results from quantitative transcriptional and proteomic analyses were documented as cell line-associated mean values  $\pm$  SD.

#### Results

A total of 121 tumours generated from 10 different HNSCC lines were analysed using bioluminescence imaging. Lactate

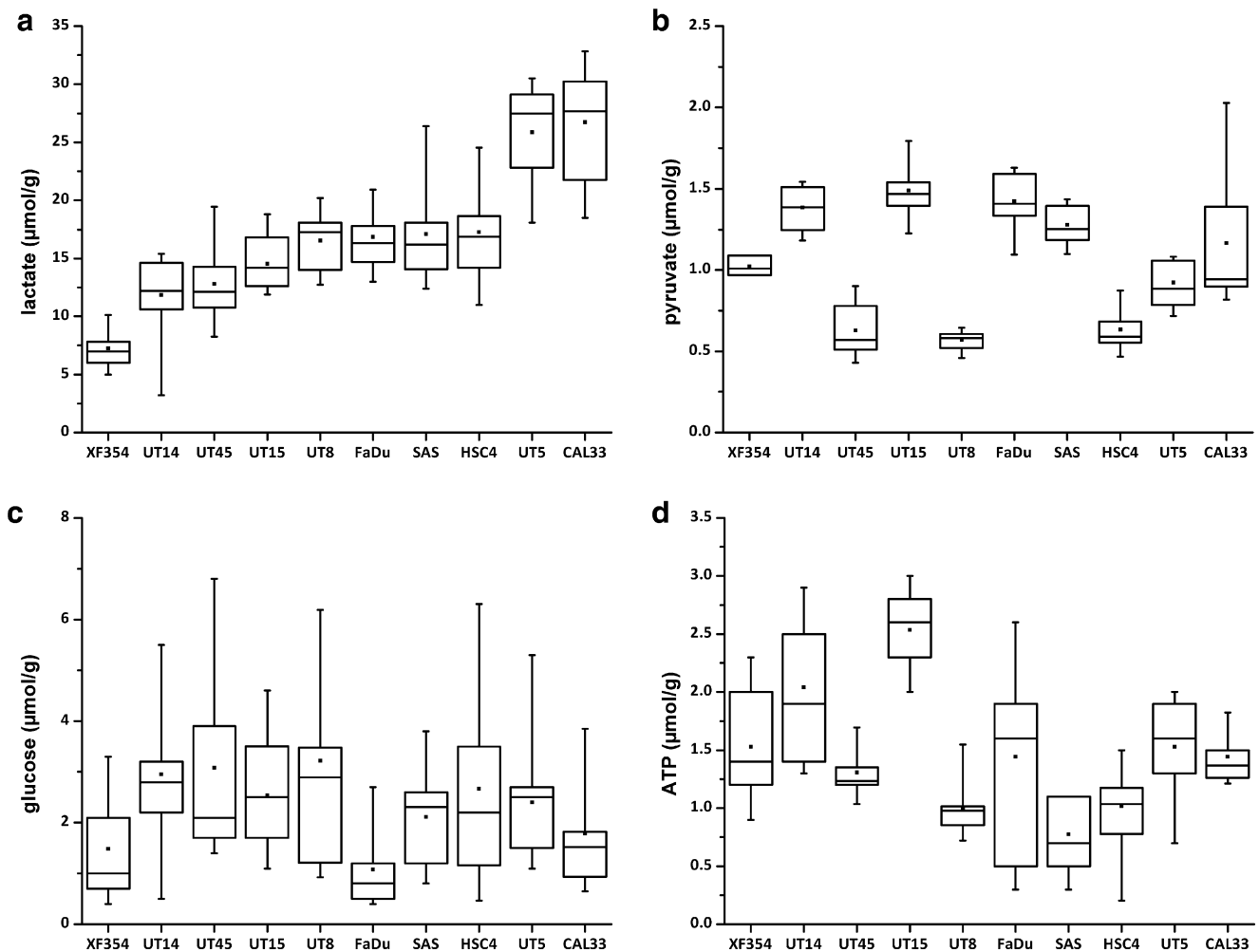


**Fig. 1.** Metabolic concentrations in human head and neck squamous cell carcinomas (HNSCCs) xenografted in nude mice measured by bioluminescence imaging. (a) Lactate concentrations were arranged in the order of ascending values. Tumour concentrations of (b) pyruvate, (c) glucose and (d) ATP in the respective xenografts are shown in the same order as in (a) for lactate.  $N = 11$ – $13$  tumours with 5–7 cryosections each for (a), (c) and (d);  $N = 11$ – $13$  tumours with 1 cryosection each for (b), except of XF354 ( $N = 3$  tumours with 2 cryosections each). Parts of the data are modified according to Quennet et al. [14]. Concentrations of all metabolites were assessed exclusively in regions with viable tumour cells. The respective tumour line-associated data are displayed as box and whiskers plots. The comparison among the data in Fig. 1a–d makes it obvious that there is no correlation between the metabolites investigated.

concentrations differed markedly between the tumour lines (Fig. 1a). Pyruvate showed rather uniform values within each tumour line (Fig. 1b) which is in contrast to glucose concentrations differing noticeably within the tumour lines (Fig. 1c). ATP concentrations also showed some variation within and between the HNSCC tumour lines (Fig. 1d). No correlations between the different metabolites were found.

Fig. 2 shows mRNA expression levels of glut1 (a) and pfk-1 (b) in the 10 investigated xenografted HNSCC tumour lines assessed by real-time RT-PCR. Expression levels were normalised to hmbs as a reference gene and to an internal calibrator. SAS showed the lowest glut1 expression which was 7.4-fold lower than that of UT-SCC-15 revealing the highest level of glut1 expression. All other tumour lines showed intermediate expression levels of glut1. The highest expression of pfk-1 was observed in UT-SCC-15 which was 7-fold higher than that in UT-SCC-5 or UT-SCC-14, respectively. Tumour glucose concentrations did not correlate with glut1 expression levels. Real-time PCR results of *ldh-a* are displayed together with the Western blot data in Fig. 3. Expression of *ldh-a* was the lowest in UT-SCC-5 compared to 7.4-fold higher expression in UT-SCC-15 which was the highest pfk-1 expression level among all tumour lines. In contrast, only minor differences in LDH-A protein expression were detected between the 10 HNSCC lines. The lowest level

of protein was found in SAS, the highest expression of LDH-A was detected in CAL-33. UT-SCC-15 showed the highest expression levels of all mRNAs investigated compared to the other tumour lines. This tumour line also showed the highest concentration of ATP and pyruvate compared to all other tumour lines, but the respective levels of lactate and glucose in this line were rather moderate. CAL-33 which revealed the highest lactate concentration of all tumour lines investigated, exhibited the highest expression of LDH-A protein. Comparable results were seen in the high lactate line UT-SCC-5 which also showed an elevated LDH-A expression. In contrast, the tumour line UT-SCC-45 which revealed the second highest amounts of LDH-A had intermediate lactate levels within the tumour lines, and SAS tumours which had a relatively high lactate concentration exhibited the lowest LDH-A expression. In essence, there was no correlation between tumour lactate concentration and any mRNA or protein expression investigated, nor was there a relationship between LDH-A mRNA and protein.

Since tumour-associated leucocytes within the xenografted tumours may contribute to lactate production and thereby to the inter-tumoural heterogeneity of lactate concentration, tumour specimens were stained for the common leucocyte antigen CD45. Representative immunohistochemical stainings of CD45 and categorisations of stained sections are given in Fig. 4. Only a few, mostly single CD45-positive cells were observed in CAL-33 (Fig. 4a) and UT-SCC-15 tumours. The highest number of CD45-positive cells was found in HSC-4 (Fig. 4b) and UT-SCC-14 tumours where larger clusters of these cells were present. The majority of the tumour sections was classified as category 1 or 2 and had low to intermediate amounts of CD45-positive cells. The percentage of leucocytes in all the tumour tissue investigated was generally low and reached a maximum of 15% in sections assessed as category 3. The two tumour lines UT-SCC-5 and CAL-33 with the highest lactate concentrations had low densities of leucocytes, while in the three tumour lines XF354, UT-SCC-14 and UT-SCC-45 with the lowest lactate concentrations higher numbers of CD45-positive cells were present. Overall, no correlation was found between the presence of tumour-infiltrating leucocytes and lactate concentration.

Measurements of lactate concentrations (mol/l cell volume per 24 h) released by the HNSCC cells *in vitro* revealed a pronounced heterogeneity between the nine cell lines. Lactate production *in vitro* did not reflect lactate concentration *in vivo*; in fact, a trend towards an inverse correlation was observed (Fig. 5): XF354 was

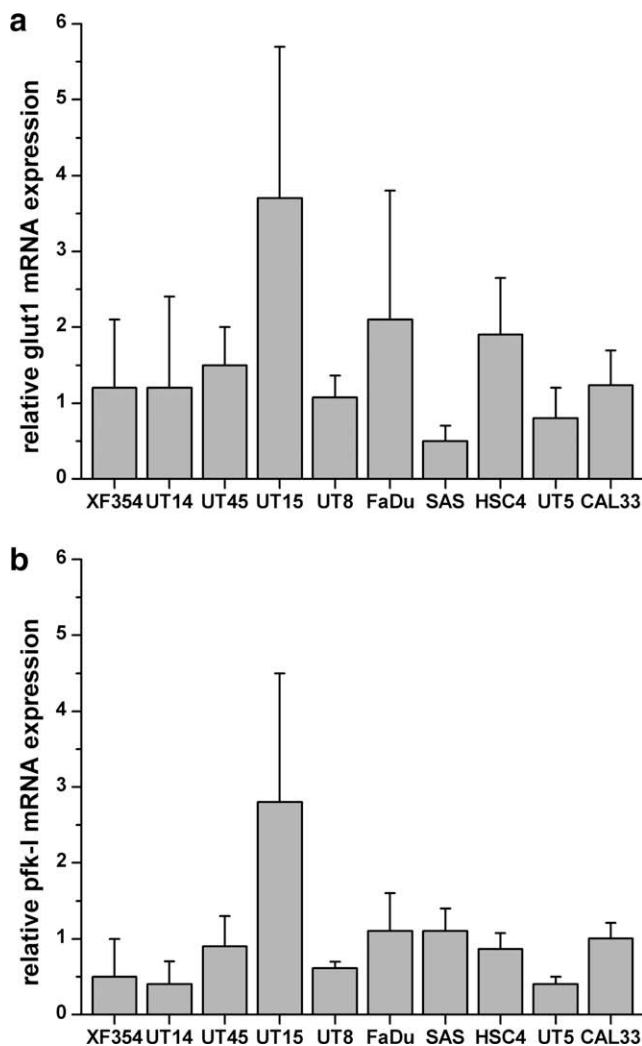


Fig. 2. Relative mRNA expression (mean + SD) of (a) glut1 and (b) pfk-1 in tumour tissues. Real-time PCR measurements were done in triplets from  $N=10-13$  tumours per tumour line which are arranged in the same order as in Fig. 1a for lactate concentrations.

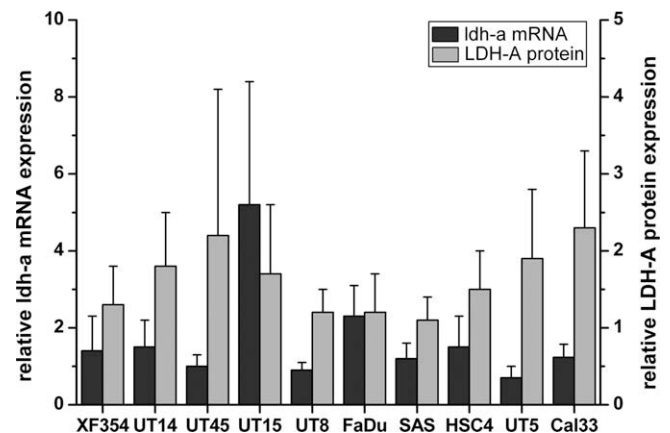
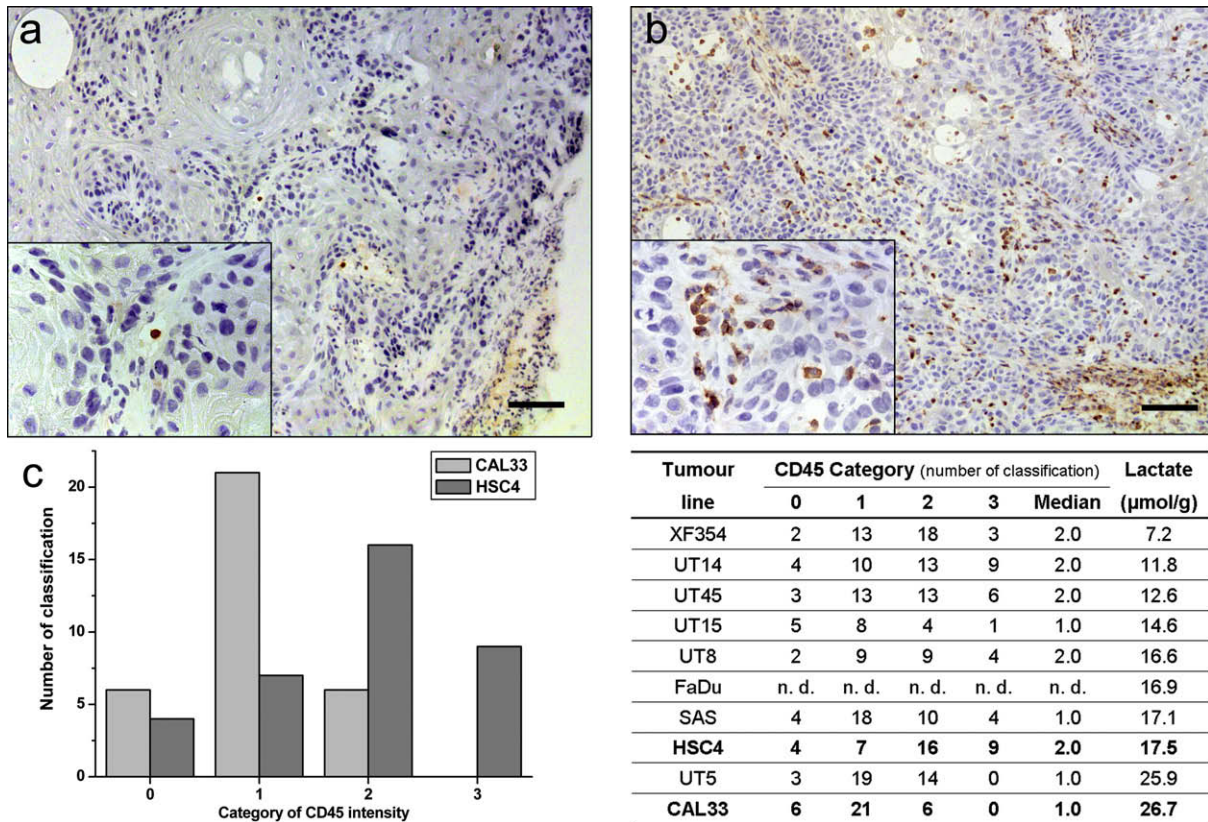


Fig. 3. Relative mRNA and protein expression (mean + SD) of lactate dehydrogenase A in tumour tissues. Real-time PCR measurements were done from  $N=10-13$  tumours per line (black columns). Western blots were done from  $N=5$  tumours per line (grey columns). Tumour lines are arranged in the same order as for lactate concentrations in Fig. 1a.



**Fig. 4.** Representative immunohistochemical stainings of tumours with (a) low CD45 expression (category 1; CAL-33) and (b) high CD45 expression (category 3; HSC-4); bars: 0.1 mm. (c) Frequency of CD45 categories in the tumour lines CAL-33 and HSC-4 was assessed independently by three investigators. Table: Summary of the results of CD45 staining; frequency of CD45 assessment in each category, median of categories, and mean lactate concentration according to Fig. 1a is given. A total number of 12 tumours with 1 section each were stained for CD45, except for UT-SCC-15 ( $n = 6$ ), UT-SCC-8 ( $n = 8$ ) and CAL-33 ( $n = 11$ ).

characterised by the highest lactate production *in vitro* and lowest lactate concentration *in vivo* compared to UT-SCC-5 which showed secondary highest lactate concentration *in vivo* and a low lactate production rate *in vitro*.

Tumour hypoxia of the xenografts investigated was determined via pimonidazole labelling and quantification of the relative hypoxic area within the viable tumour area and has been published earlier in [14,15,17]. Regression analysis of pHF values and lactate concentrations of the 10 xenografted HNSCC tumour lines revealed a weak but statistically significant correlation between these parameters (Fig. 6). Exclusion of HSC-4 which showed significant residual immune response did not change the results.

Local tumour control after fractionated irradiation was assessed in parallel experiments. Radiation response between the different tumour cell lines varied considerably with  $\text{TCD}_{50}$  values between 47.4 Gy in XF354 and 126.7 Gy in SAS tumours [16]. Lactate concentrations correlated with the  $\text{TCD}_{50}$  values after fractionated irradiation (Fig. 7a). Exclusion of HSC-4 which showed residual immune response in nude mice did not change these results.

Unexpectedly, pyruvate concentrations were not correlated with  $\text{TCD}_{50}$  values (Fig. 7b). This finding seems to refute our hypothesis of pyruvate being an efficient radical scavenger and mediator of radioresistance.

## Discussion

The current study has been focussed on possible coherencies between glycolysis, expression of glycolysis-associated proteins and response to fractionated irradiation. Data on metabolism and metabolic milieu were therefore acquired exclusively from viable tumour cell regions excluding larger stromal areas and necrosis

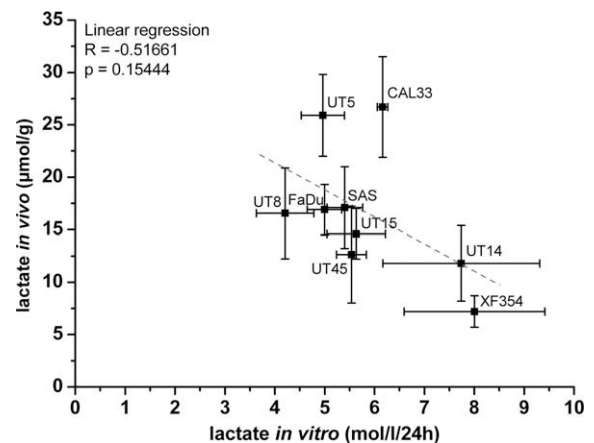


**Fig. 5.** Tumour lactate concentration *in vivo* ( $\mu\text{mol/g}$ ) as a function of lactate production *in vitro* normalised to cell volume ( $\text{mol/l/24h}$ ). Lactate production *in vitro* (mean  $\pm$  SD) was calculated in triplicates from three independent experiments, lactate concentrations *in vivo* (mean  $\pm$  SD) are shown according to Fig. 1a.

from measurement. In this way, the bioluminescence technique enabled an optical microdissection of heterogeneous tissue sections on the basis of computerised interactive image analysis. The special calibration procedure associated with this technique enables a quantitative comparison among the metabolic states of individual tumours. Furthermore, the metabolic data can be correlated with other quantitative or semi-quantitative parameters, such as therapeutic response, metastatic status, and overall and disease-free patient survival.

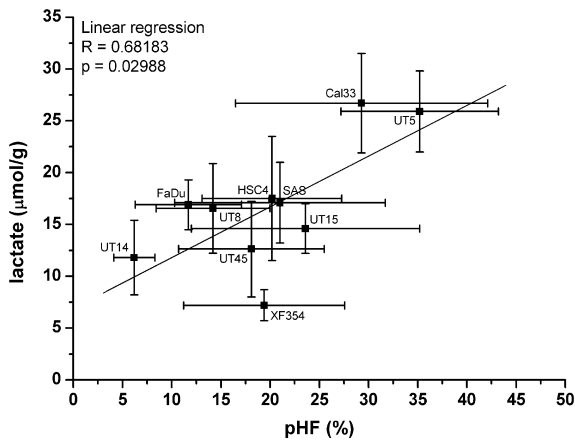


**Fig. 6.** Lactate concentration (mean  $\pm$  SD) from vital tumour regions as a function of pimonidazole hypoxic fraction, pHF (mean  $\pm$  SD), in 10 xenografted HNSCC tumour lines. Lactate concentrations and pHF were determined in 121 tumours. pHF values have been reported previously in [14,15,17]. A linear regression analysis revealed a weak but statistically significant correlation between both parameters.

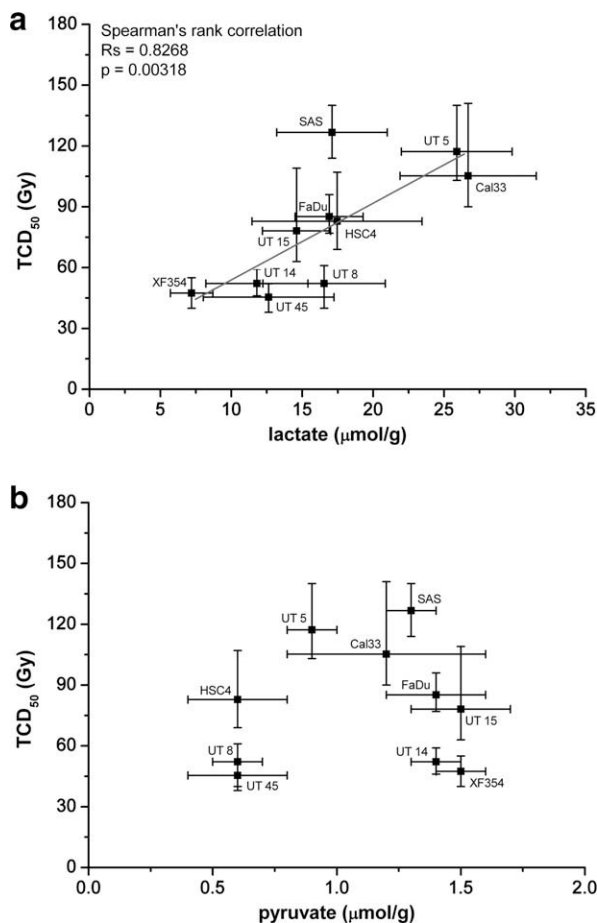


**Fig. 7.** Tumour control dose  $TCD_{50}$  (mean  $\pm$  95% confidence interval) as a function of (a) lactate and (b) pyruvate concentration (mean  $\pm$  SD) in 10 xenografted cell lines of HNSCC.  $TCD_{50}$  values [16], lactate and pyruvate concentrations were derived from 905, 121 and 101 tumours, respectively. There was a significant positive correlation only between lactate concentration within vital tumour regions and  $TCD_{50}$ . Exclusion of HSC-4 did not change this finding ( $R_s = 0.8452$ ;  $p = 0.00412$ ).

Using the bioluminescence technique in several patient studies on squamous cell carcinomas of the uterine cervix [10], of the head and neck [9] and in rectum adenocarcinomas [24], a high lactate

concentration in primary lesions at first presentation in the clinic was identified to predict for a high probability of metastasis formation and a restricted patient survival [25,26]. Specifically, for HNSCCs, the entity investigated in the current study, these lactate concentrations were lower with patients surviving  $\geq 3$  years compared to the non-survivor group at a significance level of  $p < 0.0001$ . Since the majority of these HNSCC patients had received a standard radiotherapy, the difference in survival between patients with high and low lactate tumours may be, at least partially, attributable to lactate-associated radioresistance. As a consequence, the working hypothesis of the current investigation was that high pre-therapeutic lactate accumulation in primary tumours may indicate a pronounced therapeutic resistance, in particular to ionizing radiation. However, this does not necessarily mean that lactate by itself confers radioresistance to cells; lactate may rather be an indicator of a high turnover rate in the glycolytic pathway. This important issue is currently under investigation in our laboratories. Preliminary findings show that mimicking the metabolic environment *in vivo* during an irradiation experiment *in vitro* requires a series of systematic and sophisticated experiments. It seems not sufficient to simply irradiate cells in media with high lactate concentrations ignoring the characteristics of the cell line or the impact of pH, hypoxia, energetic status and many other parameters [27].

Regardless of the underlying mechanism, the data presented here on lactate concentration and  $TCD_{50}$  in 10 tumour lines including more than 1000 individual tumours clearly demonstrate the phenomenon of lactate being predictive of radiation resistance. Thus, the poor outcome for patients with high lactate malignancies in the clinical studies mentioned might at least be partially due to glycolysis-mediated resistance to radiotherapy. Manipulation of glycolysis to alter the levels of antioxidant metabolites, such as lactate and pyruvate, might therefore lead to a better therapy response, and is a promising avenue for further research. Interfering with the glycolytic phenotype of tumour cells may be achieved at the level of glycolysis or associated pathways. There are a number of investigations on shifting tumour cell metabolism from glycolysis to glucose oxidation by the inhibition of LDH activity as well as by the up-regulation of pyruvate dehydrogenase (PDH) activity. Either approach is thought to reduce lactate production and force pyruvate oxidation and can be achieved via biochemical inhibitors or via knockdown of enzyme expression levels; however, most of these studies are on the pre-clinical level and are not yet tested in patients [28]. It has been shown by several studies that an up-regulated glycolytic activity of tumours is associated with a malignant phenotype, resistance to chemo- and radiotherapy, and ultimately with a poor prognosis. Our findings might also have clinical implications as non-invasive techniques for imaging and quantifying lactate in tumours are available [29–31]. Proton magnetic resonance spectroscopic imaging (MRSI) is one of these techniques which has been shown to be suitable for monitoring tumour response to radiotherapy [32], for pre-surgical grading of tumours [33], and for the prognosis of patient survival [34] on the basis of lactate imaging. The data given in Fig. 7a may imply that non-invasive lactate measurement by MRSI may be used in patients to predict response to radiation.

One candidate glycolytic metabolite which may be directly involved in the generation of radiation resistance is pyruvate. This carbonic acid can be reduced non-enzymatically to acetate, thereby scavenging hydrogen peroxide [12]. In a Fenton reaction in the presence of iron, the latter is a source of hydroxyl radicals which ultimately mediate the fixation of radiation-induced DNA damage. Unexpectedly, the findings with regard to pyruvate in relation to  $TCD_{50}$  clearly show that the tumour pyruvate concentration is not correlated with radiosensitivity. This is surprising, since there is a substantial variability in pyruvate between tumour lines, albeit

the absolute levels are in general relatively low compared to those of lactate. Since pyruvate concentrations are mostly dependent on the expression and the activation levels of LDH and PDH, different activities between the tumour lines may lead to variations in pyruvate contents. We could not detect a correlation between LDH-A protein expression and pyruvate concentrations, suggesting that pyruvate metabolism is rather regulated through PDH activity in the tumour lines investigated. The same is true for the finding that lactate concentrations and LDH-A mRNA and protein levels did not correlate in the tumour lines. Pure expression levels apparently do not give sufficient information on the activation status of an enzyme and on regulation mechanisms. Therefore measuring enzyme activities might give more plausible results. Unfortunately, due to missing quantitative technologies, enzyme activities are currently difficult to determine *in vivo* or in cryobiopsies.

We found no correlation between single cell lactate production rates *in vitro* and lactate concentration *in vivo*. This may be explained by different lactate production rates *in vivo* versus *in vitro*. In addition, the tumour microenvironment may affect lactate concentrations *in vivo*. One important environmental factor, besides hypoxia, is the glucose availability which is variable and largely restricted in tumours with local glucose concentrations being far below arterial blood levels. In contrast, the measurements of cellular lactate production *in vitro* were performed in media containing glucose concentrations of five times that of normal blood. Ongoing mechanistic studies in our laboratories indicate that the relationship between external glucose concentration, cellular glucose uptake and lactate release is rather complex, since lactate may be recruited not only from glucose but also from pyruvate and amino acids, such as glutamine and alanine [35]. Similarly, the missing correlation between the expression of glycolysis-associated transporters or enzymes and metabolism is representing a further gap in knowledge with regard to mechanisms inducing such a large variance in tumour lactate levels. This is true for malignancies that are very similar in all other biological and clinical aspects accessible at the moment. We also suggest that, due to differences within the methodical approaches used, discrepancies between the *in vitro* and *in vivo* models can be explained. The technique of bioluminescence imaging does not distinguish between extracellular and intracellular metabolites. Thus, besides intracellular lactate, lactate that is transported out of the cell can be monitored, as long as it is not removed by the blood flow. In contrast, *in vitro* measurements of lactate production exclusively account for extracellular lactate. Another aspect could be the composition of cell culture media. Since common media contain high concentrations of L-glutamine and pyruvate which may also contribute to lactate production *in vitro*, and since besides glycolysis, glutaminolysis is another main source for energy production and seems to contribute to elevated lactate accumulation in tumour cells [35], comparison between *in vitro* and *in vivo* models with regard to their metabolic status is highly complex. Despite a lack of knowledge of the underlying mechanisms *in vitro*, the major focus of the present study was the identification of metabolic parameters for the prediction of radiosensitivity in solid tumours *in vivo*.

Our results revealed a weak but statistically significant correlation between pHF and lactate concentrations in the HNSCC xenografts (Fig. 6) which might suggest higher glycolytic flux or higher accumulation of lactate in hypoxic areas. Earlier studies on five of the 10 tumour lines illustrate that tumour areas positive for pimonidazole were almost exclusively located distant from perfused vessels [15]. Most recently, Yaromina et al. showed in three tumour lines also included in the present investigation that at the microregional level high lactate concentrations were not associated with hypoxia but with low perfusion [36]. In light of these

findings our results suggest that both hypoxia and lactate accumulation are associated with low perfusion. Pronounced lactate accumulation may thus be governed predominantly by a restricted clearance potential at least in some tumours.

In a simulation multivariate analysis, pHF and lactate were found to be independent prognostic factors for local tumour control after fractionated irradiation (Zips et al., unpublished data, manuscript in preparation).

It has been demonstrated that leucocytes can produce significant amounts of lactate at sites of sepsis [37]. Therefore an analysis of leucocyte infiltration in the xenografted tumours that could influence lactate production seemed necessary. Evaluation of CD45 staining as a marker revealed some differences between nine tumour lines. One of the lines with overall highest rating was HSC-4 which has been shown to evoke a significant residual immune response in nude mice [16]. However, the overall amount of CD45-positive cells in the tumour tissue was low and did not exceed 15% of total cell numbers. This result together with the fact that the two tumour lines with highest lactate concentrations (UT-SCC-5 and CAL-33) had low densities of CD45-positive cells, suggests that infiltrating leucocytes are not a major source of lactate in the tumours analysed in this study.

We found pronounced heterogeneity in metabolite concentrations across the xenograft lines investigated. This could be ascribed neither to the cellular lactate production rate or expression level of enzymes, nor to infiltration of lactate-producing immune cells. The only positive correlation for lactate was found with the pimonidazole hypoxic fraction, which we interpreted as being caused by an association of both parameters with low perfusion. Since each population of cancer cells is influenced by numerous factors, such as oxygenation status, glucose supply and consumption rate, vascularisation, intra- and extracellular pH values, expression levels of oncogenes and their downstream targets, furthermore extended investigations into multiple parameters appear necessary to unravel the mechanisms by which metabolic and microenvironmental factors influence radioresistance and to identify promising targets for specific interventions. Furthermore, our data indicate that such investigations should also attempt to analyse the interrelationship of tumour hypoxia, perfusion and metabolic environment with a focus on the activation level of enzymes.

In summary, lactate but not pyruvate concentration correlates with tumour response after fractionated irradiation in HNSCC xenografts. Obviously, lactate accumulates in highly aggressive and radioresistant tumours, whereas pyruvate does not accumulate to this extent, but may be rather rapidly metabolised through various enzymes involved in different metabolic pathways. The mechanisms underlying these effects appear complex and necessitate further research. Nevertheless, lactate imaging to monitor therapy response and the combination of radiotherapy with the inhibitors of glycolysis appear promising avenues for translational pre-clinical and clinical studies.

## Acknowledgements

The authors thank E. Wenzel, S. Balschukat, D. Pfitzmann, K. Schumann and M. Oelsner for excellent technical assistance. The authors would also like to thank Dr. C. Bayer for the preparation of protein extracts from xenograft samples and S. Krato for the measurements of lactate production rates in XF354, FaDu and UT-SCC-5.

*Financial support:* This investigation was supported by grants of the Deutsche Forschungsgemeinschaft (DFG) to W.M.K. (Mu 576/14-2; 14-3) and to M.B. and D.Z. (Ba 1433/4-2), German Federal Ministry of Education and Research to M.B. and D.Z. (BMBF 03ZIK/OncoRay) and in parts by a grant of the Stiftung Rheinland-Pfalz für Innovation to W.M.K. (15202-386261/606).

## References

- [1] Rajendran JG, Mankoff DA, O'Sullivan F, et al. Hypoxia and glucose metabolism in malignant tumors: evaluation by [18F]fluoromisonidazole and [18F]fluorodeoxyglucose positron emission tomography imaging. *Clin Cancer Res* 2004;7:2245–52.
- [2] Zu XL, Guppy M. Cancer metabolism: facts, fantasy, and fiction. *Biochem Biophys Res Commun* 2004;3:459–65.
- [3] Atsumi T, Chesney J, Metz C, et al. High expression of inducible 6-phosphofructo-2-kinase/fructose-2,6-bisphosphatase (iPFK-2; PFKFB3) in human cancers. *Cancer Res* 2002;20:5881–7.
- [4] Gatenby RA, Gillies RJ. Why do cancers have high aerobic glycolysis? *Nat Rev Cancer* 2004;11:891–9.
- [5] Semenza GL. HIF-1 and tumor progression: pathophysiology and therapeutics. *Trends Mol Med* 2002;4:S62–7.
- [6] Warburg O. Origin of cancer cells. *Science* 1956;3191:309–14.
- [7] Schwickert G, Walenta S, Sundfor K, Rofstad EK, Mueller-Klieser W. Correlation of high lactate levels in human cervical cancer with incidence of metastasis. *Cancer Res* 1995;21:4757–9.
- [8] Walenta S, Salameh A, Lyng H, et al. Correlation of high lactate levels in head and neck tumors with incidence of metastasis. *Am J Pathol* 1997;2:409–15.
- [9] Brizel DM, Schroeder T, Scher RL, et al. Elevated tumor lactate concentrations predict for an increased risk of metastases in head-and-neck cancer. *Int J Radiat Oncol Biol Phys* 2001;2:349–53.
- [10] Walenta S, Wetterling M, Lehrke M, et al. High lactate levels predict likelihood of metastases, tumor recurrence, and restricted patient survival in human cervical cancers. *Cancer Res* 2000;4:916–21.
- [11] Groussard C, Morel I, Chevanne M, et al. Free radical scavenging and antioxidant effects of lactate ion: an in vitro study. *J Appl Physiol* 2000;1:169–75.
- [12] Salahudeen AK, Clark EC, Nath KA. Hydrogen peroxide-induced renal injury. A protective role for pyruvate in vitro and in vivo. *J Clin Invest* 1991;6:1886–93.
- [13] Brown JM, Wilson WR. Exploiting tumour hypoxia in cancer treatment. *Nat Rev Cancer* 2004;6:437–47.
- [14] Quennet V, Yaromina A, Zips D, et al. Tumor lactate content predicts for response to fractionated irradiation of human squamous cell carcinomas in nude mice. *Radiother Oncol* 2006;2:130–5.
- [15] Yaromina A, Zips D, Thames HD, et al. Pimonidazole labelling and response to fractionated irradiation of five human squamous cell carcinoma (hSCC) lines in nude mice: the need for a multivariate approach in biomarker studies. *Radiother Oncol* 2006;2:122–9.
- [16] Yaromina A, Krause M, Thames H, et al. Pre-treatment number of clonogenic cells and their radiosensitivity are major determinants of local tumour control after fractionated irradiation. *Radiother Oncol* 2007;3:304–10.
- [17] Yaromina A, Holscher T, Eicheler W, et al. Does heterogeneity of pimonidazole labelling correspond to the heterogeneity of radiation-response of FaDu human squamous cell carcinoma? *Radiother Oncol* 2005;2:206–12.
- [18] Bayer C, Schilling D, Hoetzel J, et al. PAI-1 levels predict response to fractionated irradiation in 10 human squamous cell carcinoma lines of the head and neck. *Radiother Oncol* 2008;3:361–8.
- [19] Baumann M, Krause M, Hill R. Exploring the role of cancer stem cells in radioresistance. *Nat Rev Cancer* 2008;7:545–54.
- [20] Mueller-Klieser W, Walenta S. Geographical mapping of metabolites in biological tissue with quantitative bioluminescence and single photon imaging. *Histochem J* 1993;6:407–20.
- [21] Sattler UG, Walenta S, Mueller-Klieser W. A bioluminescence technique for quantitative and structure-associated imaging of pyruvate. *Lab Invest* 2007;1:84–92.
- [22] Lallemand B, Evrard A, Combescure C, et al. Reference gene selection for head and neck squamous cell carcinoma gene expression studies. *BMC Mol Biol* 2009;1:78.
- [23] Yaromina A, Eckardt A, Zips D, et al. Core needle biopsies for determination of the microenvironment in individual tumours for longitudinal radiobiological studies. *Radiother Oncol* 2009;3:460–5.
- [24] Walenta S, Chau T-V, Schroeder T, et al. Metabolic classification of human rectal adenocarcinomas: a novel guideline for clinical oncologists? *J Cancer Res Clin Oncol* 2003;6:321–6.
- [25] Walenta S, Mueller-Klieser WF. Lactate: mirror and motor of tumor malignancy. *Semin Radiat Oncol* 2004;3:267–74.
- [26] Walenta S, Schroeder T, Mueller-Klieser W. Lactate in solid malignant tumors: potential basis of a metabolic classification in clinical oncology. *Curr Med Chem* 2004;16:2195–204.
- [27] Grotius J, Dittfeld C, Huether M, et al. Impact of exogenous lactate on survival and radioresponse of carcinoma cells in vitro. *Int J Radiat Biol* 2009;11:989–1001.
- [28] Cuezva JM, Ortega AD, Willers I, et al. The tumor suppressor function of mitochondria: translation into the clinics. *Biochim Biophys Acta* 2009.
- [29] Melkus G, Morchel P, Behr VC, et al. Short-echo spectroscopic imaging combined with lactate editing in a single scan. *NMR Biomed* 2008;10:1076–86.
- [30] Brindle K. New approaches for imaging tumour responses to treatment. *Nat Rev Cancer* 2008;2:94–107.
- [31] Plathow C, Weber WA. Tumor cell metabolism imaging. *J Nucl Med* 2008;43S–63S.
- [32] Laprie A, Pirzkall A, Haas-Kogan DA, et al. Longitudinal multivoxel MR spectroscopy study of pediatric diffuse brainstem gliomas treated with radiotherapy. *Int J Radiat Oncol Biol Phys* 2005;1:20–31.
- [33] Raizer JJ, Koutcher JA, Abrey LE, et al. Proton magnetic resonance spectroscopy in immunocompetent patients with primary central nervous system lymphoma. *J Neurooncol* 2005;2:173–80.
- [34] Xu M, See SJ, Ng WH, et al. Comparison of magnetic resonance spectroscopy and perfusion-weighted imaging in presurgical grading of oligodendroglial tumors. *Neurosurgery* 2005;5:919–26.
- [35] DeBerardinis RJ, Sayed N, Ditsworth D, Thompson CB. Brick by brick: metabolism and tumor cell growth. *Curr Opin Genet Dev* 2008;1:54–61.
- [36] Yaromina A, Quennet V, Zips D, et al. Co-localisation of hypoxia and perfusion markers with parameters of glucose metabolism in human squamous cell carcinoma (hSCC) xenografts. *Int J Radiat Biol* 2009;11:972–80.
- [37] Haji-Michael PG, Ladriere L, Sener A, Vincent JL, Malaisse WJ. Leukocyte glycolysis and lactate output in animal sepsis and ex vivo human blood. *Metab Clin Exp* 1999;6:779–85.